



Article

# Lightweight Structural Concepts in Bearing Quasi-Static Ice Hull Interaction Loads

Harsha Cheemakurthy \* , Zuheir Barsoum, Magnus Burman and Karl Garne 

Department of Engineering Mechanics, KTH Royal Institute of Technology, 114 28 Stockholm, Sweden; zuheir@kth.se (Z.B.); mburman@kth.se (M.B.); garne@kth.se (K.G.)

\* Correspondence: harsha@kth.se

**Abstract:** Lightweight ice-class vessels offer the possibility of increasing the payload capacity while making them comparable in energy consumption with non-ice-class vessels during ice-free periods. We approach the development of a lightweight hull by dividing ice–hull interactions into quasi-static loading and impact loading phases. Then, investigative outcomes of lightweight concepts for each loading phase may be combined to develop a lightweight ice-going hull. In this study, we focus on the quasi-static loading phase characteristic of thin first-year ice in inland waterways. We investigate metal grillages, sandwich structures and stiffened sandwich structures parametrically using the finite element method. The model is validated using previous experimental studies. In total over 2000 cases are investigated for strength and stiffness with respect to mass. The stiffened sandwich was found to be the most favorable concept that offered both a light weight as well as high gross tonnage. Further, significant parameters and their interactions and material differences for the three structural concepts were investigated and their trends discussed. The outcomes result in the creation of a viable pool of lightweight variants that fulfill the quasi-static loading phase. Together with outcomes from the impact loading phase, a lightweight ice-going hull may be developed.

**Keywords:** composites; sandwich; metal grillage; aluminum hull; ice loads; finite element method; urban waterborne mobility; inland waterways



**Citation:** Cheemakurthy, H.; Barsoum, Z.; Burman, M.; Garne, K. Lightweight Structural Concepts in Bearing Quasi-Static Ice Hull Interaction Loads. *J. Mar. Sci. Eng.* **2022**, *10*, 416. <https://doi.org/10.3390/jmse10030416>

Academic Editors: Selda Oterkus, Erkan Oterkus and Murat Ozdemir

Received: 20 February 2022

Accepted: 7 March 2022

Published: 13 March 2022

**Publisher's Note:** MDPI stays neutral with regard to jurisdictional claims in published maps and institutional affiliations.



**Copyright:** © 2022 by the authors. Licensee MDPI, Basel, Switzerland. This article is an open access article distributed under the terms and conditions of the Creative Commons Attribution (CC BY) license (<https://creativecommons.org/licenses/by/4.0/>).

## 1. Introduction

Navigation in ice-covered inland waterways is important from an economic and mobility standpoint. The current state of the art for designing ice-class vessels relies on rule-based design which recommends steel as the hull material [1–3]. In comparison with non-ice inland-waterway vessels, the ice-classed vessels' larger scantlings put them at a disadvantage in terms of energy consumption and payload during non-ice periods. A degree of parity could be achieved by switching to lightweight hulls that are safe for ice operations.

Several articles in research can be found towards the reduction of steel hull weight. Pavic, Daley [4] and Daley and Hermanski [5] concluded having multiple frames results in up to a 35% higher post-yield capacity than a single frame. The larger capacity could be the basis for reducing the weight by decreasing the scantlings for a lower probability of exceedance of ice thickness. Cheemakurthy, Zhang [6] studied the non-linear structural behavior of barges and noted the beneficial effects of strain hardening in reducing the structural scantlings. Abraham [7] study on different stiffener cross-sections showed flat bar stiffeners to be most weight-efficient. Avellan [8] investigation showed transversely stiffened hulls are more weight-efficient in comparison to longitudinally stiffened hulls. A thorough parametric study would help identify sensitive parameters and lead to a more efficient conventional design.

Steel as a hull material in ice-going vessels is justified considering its toughness against the stochastic nature of ice–hull interaction fuelled by the lack of absolute theoretical models

and reliance on expensive full-scale tests with adjustments for risk [9]. We can limit the stochasticity by considering thin first-year ice and assuming proper route planning. This justifies the exploration of alternative materials and structural concepts.

Crum, McMichael [10] studied applications for aluminum alloy aboard naval vessels and observed good survivability in extreme working conditions and impact resistance. Herrnring, Kubiczek [11] performed ice drop tests on an aluminum grillage and observed structural integrity, however, with some plastic deformations. Kujala and Klanac [12] studied steel sandwich panels and noted structural weight savings of 30–50%.

In exploring alternative structural concepts, fibre reinforced plastic (FRP) sandwich structures represent potential owing to their previous applications in extreme conditions in a naval environment including mild ice operations [13]. Not only have they demonstrated potential for impact resistance [14], they also have high bending strength to density ratio, making them a good candidate for bearing large quasi-static loads [15], typical in ice–hull interactions. In non-ice operations, speed boats with high slamming loads have been built with composites and have shown good performance [16,17]. In view of increasing the gross tonnage of the vessel, a combination of sandwich panels and stiffeners called the stiffened sandwich is worth exploring. Goel, Matsagar [18] explored this concept with different stiffener orientations and noted that rectangular stiffeners performed better and suggested placement of stiffeners under the load patch.

In our goal towards the conceptual development of the lightweight ice going hull, we envisage the hull to be a composite of 3 layers, each corresponding to the three stage of ice–hull interactions: impact-crushing phase, bending-breaking phase and displacement phase [19]. In this paper we focus on the bending phase for which we assume quasi-static loading. The other phases are explored in subsequent studies.

We note that previous studies have largely focussed on specific cases and their implications on ice navigation are not understood very well. Hence, this motivates the current study where we perform a parametric study and assess the strength and stiffness of three structural concepts—metal grillages, sandwich structures and stiffened sandwich structures under thin first-year ice loads. The concepts are parametrized geometrically and by material. We use a commercial finite element method (FEM) software for the investigations. Respective FEM models are validated using experimental studies for metal grillages [20] and sandwich panels [21].

The respective outcomes of the analysis will answer which is the most suitable lightweight structural concept for the quasi-static phase of ice–hull interactions. Further, the outcomes will highlight sensitive parameters and parametric interactions for each structural concept, potentially leading to weight-efficient design.

## 2. Proposed Hull Concepts and Candidates

### 2.1. Ice–Hull Interaction Scenarios

Ice operations may include direct and indirect collisions with ice, advancement in level ice and ice fields with ridges, brash ice and vessels jamming in between two compressive ice fields [22]. Since the scope of the current study is limited to thin first-year freshwater ice typically found in Lake Mälaren, Sweden, ice–hull interactions can be reduced to advancement in level ice and brash ice. Assuming a 95% operational time window, the maximum ice thickness is 50 cm (noted from the Swedish meteorological and hydrological institute [23]).

For level ice, the typical ice–hull interaction can be broken down into three phases as shown in Figure 1a [19,24,25]. The interaction schematic and the loading curve in Figure 1b show a large peak corresponding to the flexural failure of ice while the smaller high-pressure peaks correspond to spalling, fracturing and extrusion of material [26]. The ice flexural failure mechanism can be assumed as quasi-static based on FSICR recommendations for direct calculations and previous literature studies [27,28].

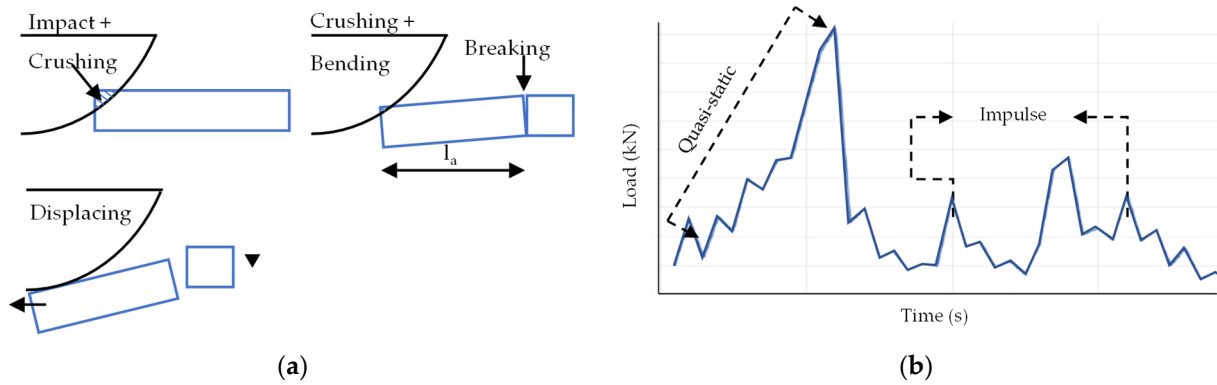


**Figure 1.** (a) Hull–ice interaction mechanism and (b) Within the associated ice loading pattern, flexural bending is assumed to be quasi-static while spalling, fracturing and material extrusion loads are assumed to be dynamic.

In isolation, the quasi-static assumption may not completely represent ice–hull interactions, but by also considering dynamic loading (planned for future work), we may capture the ice loading reasonably. This motivates the introduction of the proposed hull concept in the next sub-section.

2.2. Proposed Concept for Hull Panel

The lightweight hull structure that we envisage must bear loads relating to the three stages of ice–hull interactions. Correspondingly, in Figure 2 we envisage the structural concept as a composite of three layers where the outermost layer is abrasion-resistant (L1), the layer underneath is dynamic loading and impact-resistant (L2), and the innermost layer can withstand large quasi-static forces (L3). While layer L1 disperses impulse loads within high-pressure zones, L2 bears the large resulting pressures that follow. We examine only quasi-static loads in this study and the other phases are investigated in subsequent studies. The structural concepts for this study are compiled in Table 1. The large uncertainties arising from ice load evaluation methods [29] could be overcome by considering all ice-interaction modes.

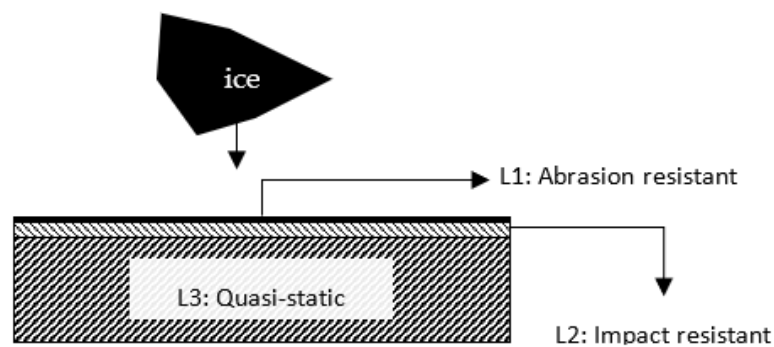


**Figure 2.** Proposed structural concept for an ice-going hull consists of three layers specialized in handling quasi-static loads (L3), dynamic loads (L2) and abrasion due to ice scraping (L1).

**Table 1.** Structural concepts and respective materials that are investigated in this study.

Structural Concept		Material	
Metal grillage		Structural Steel Aluminium alloy	
Sandwich	Face:	Carbon fibre epoxy 230 GPa UD Carbon fibre epoxy 395 GPa UD, woven Glass fibre epoxy	Core: PVC 60, 200 PET 200, 320
Stiffened sandwich	Face and stiffeners:	Carbon fibre epoxy 230 GPa UD Carbon fibre epoxy 395 GPa UD, woven Glass fibre epoxy	Core: PVC 60, 200 PET 200, 320

### 2.3. Structural Concepts

The structural concepts are chosen considering the potential for lightweight and prevalent state-of-the-art in marine construction. Starting with metal grillages, FSICR [1] recommends the use of steel which we incorporate in this study to set a reference for comparison. In addition, we investigate aluminum alloy owing to its known performance in extreme working conditions aboard naval ships [10] and ice impact survivability [11]. The second structural concept in the study is sandwich structures which have found application in the marine industry [16,17]. Further, Mouritz, Gellert [13] have observed the application of the concept in Swedish naval vessels operating in extreme conditions including light ice. The final structural concept under investigation is the stiffened sandwich panel. The concept is a combination of a sandwich structure with the inner face sheet consisting of FRP stiffeners. This concept [18] allows lower core thickness that increases the gross tonnage while having comparable strength with a sandwich.

For the sandwich face material, we compared two contemporary materials—carbon fibre and E-glass. For carbon fibre, we included the 230 GPa variant and the 395 GPa variant oriented as (a) uni-directional (UD) fibres and (b) woven fabric. For the core material, we considered Balsa wood, honeycomb, PVC and PET. However, owing to the difficulties of waterlogging in the event of panel penetration, we study only closed-cell foams with varying densities.

### 2.4. Geometric Parametrization

To facilitate this study, critical geometric elements are identified and parametrized around initial values calculated using analytical models, rule-based design [2] and practical aspects. Figure 3 and Table 2 show respective parameters where three variants of each parameter are implemented leading to a total of 3<sup>n</sup> cases for each structural concept. Respective material properties for the structural concepts are shown in Table 3.

**Table 2.** Parametrization of structural concepts.

Structural Concept	Structural Element	Variants
Metal Grillage (486 cases)	Plate thickness	10, 15, 20 mm
	Stiffener spacing	0.25, 0.5, 0.67 m (0.67 m: no ice stiffener)
	Stringer spacing	0.5, 0.67, 1 m (0.67 m: no ice stringer)
	Stiffener elastic section modulus	18.4, 57.3, 94.8 cm <sup>3</sup>
	Stringer elastic section modulus	150, 303, 443 cm <sup>3</sup>
	Materials	Steel, Aluminum
Sandwich Structure (405 cases)	Face single ply thickness	0.2, 0.3, 0.4 mm
	Thin core thickness	75, 175, 275 mm
	Thick Core thickness	300, 450, 600 mm
	Face ply angles	[+45/−45] <sub>s</sub> ; [+90/0] <sub>s</sub> ; [90/0/45/−45/45/−45/0/90] <sub>s</sub>
	Face materials	Carbon fibre 235, Carbon fibre 395, E-glass
	Core materials	PVC 60/200, PET 200/320
Stiffened Sandwich Structure (1215 cases)	Face single ply thickness	0.2, 0.3, 0.4 mm
	Thick Core thickness	150, 275, 400 mm
	Thin Core thickness	60, 100, 140 mm
	Face ply angles	[90/0/45/−45/45/−45/90/0] <sub>s</sub>
	Plate and stiffener face materials	Carbon fibre 235, Carbon fibre 395, E-glass
	Plate core materials	PVC 60/200, PET 200/320
	Elastic Section modulus stiffener	18.4, 57.3, 94.8 cm <sup>3</sup>
Stiffener spacing	0.25, 0.5, 0.67 m	

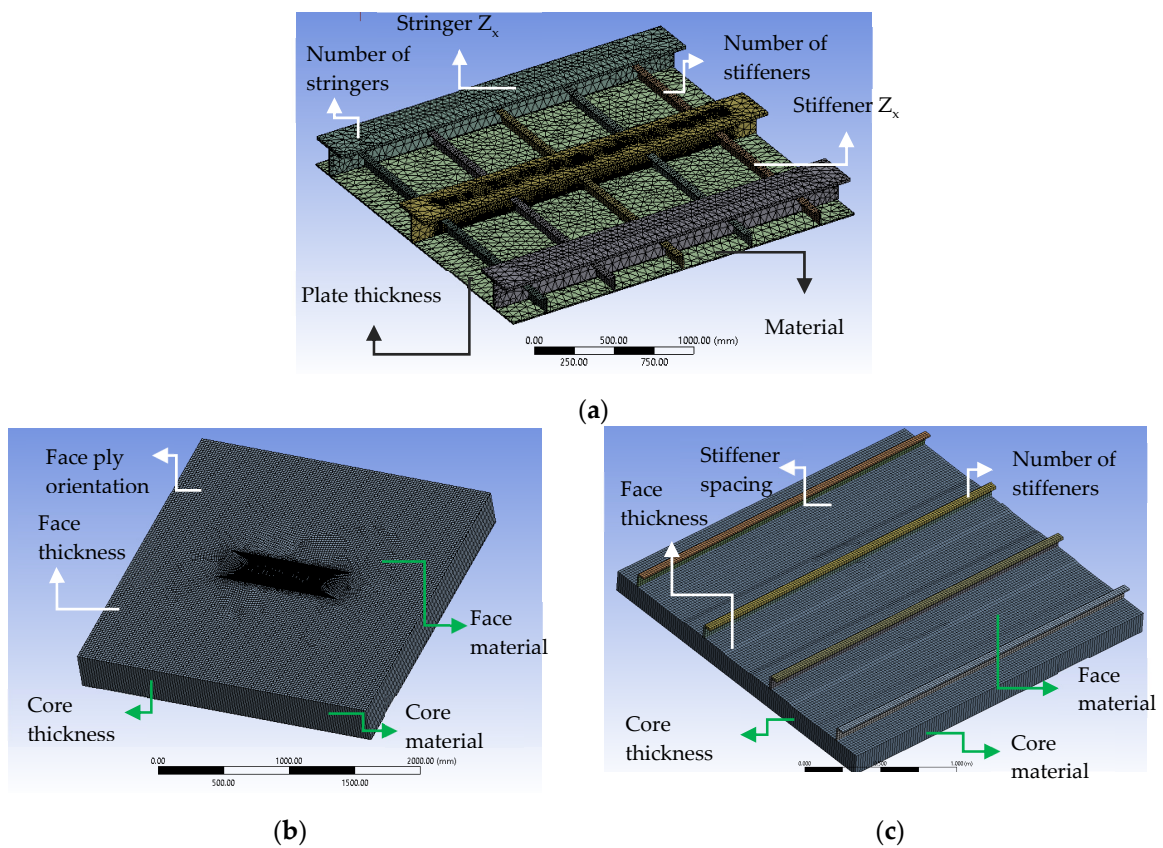


**Figure 3.** Parametrization of (a) metal grillage, (b) sandwich panel and (c) stiffened sandwich panel.

For steel grillages, ice-class rules for class 1B following FSICR (2021) were used to deduce initial scantlings and define the upper parametric limit. The lower limit was taken as per inland navigation rules [30]. For aluminum alloy, we used similar scantlings since there are no rules for this material. The girders have a T cross-section while the stiffeners have an L cross-section. The choice of parameters for the FRP composite was deduced using the constant stiffness design method [31]. The structural design calculations for a panel of dimensions  $2.4\text{ m} \times 2.4\text{ m}$  with a pressure patch representing ice pressure given by FSICR (2021) in the middle were performed. We minimized the structure for mass with constraints for stiffness  $w/b \leq 0.02$  and strength  $\sigma_{f,max} = E_f/64$  [32]. The resulting face and core thicknesses were used as a reference to decide the parameters. For the stiffened sandwich, a similar approach was used where the face sheet and core thicknesses are deduced. The stiffener section moduli were chosen to correspond to the metal grillage to create a basis for comparison.

**Table 3.** Properties of materials used in the parametrization of structural candidates.

Material	Density (kg/m <sup>3</sup> )	Young's Modulus (MPa)	Shear Modulus (MPa)	Tensile/Shear Yield Strength (MPa)	Tensile Ultimate Strength (MPa)	Orthotropic Strain Limit
Structural Steel [33,34]	7850	2e5	7.69e4	250	460	
Aluminum alloy [35]	2770	7.1e4	2.67e4	280	310	
Carbon fibre 230 [33]	1490	X: 1.21e5 Y, Z: 8600	XY, XZ: 4700 YZ: 3100	X: 2231 Y, Z: 29		Y, Z: 0.0032 X: 0.0167
Carbon fibre 395 [33]	1540	X: 2.09e5 Y, Z: 9450	XY, XZ: 5500 YZ: 3900	X: 1979 Y, Z: 26		Y, Z: 0.0031 X: 0.0092
E-glass [33]	2000	X: 4.5e4 Y, Z: 1e4	XY, XZ: 5000 YZ: 3846.2	X: 1100 Y, Z: 35		Y, Z: 0.0035 X: 0.0244
PVC60 [33]	60	70	26.9	1.5 (tensile) −1.5 (compressive) 0.93 (shear)		
PVC200 [36]	200	175	75	6 (tensile) −5.2 (compressive) 3.5 (shear)		
PET GR200 [37]	200	235	51	3.9 (tensile) −4 (compressive) 1.75 (shear)		
PET GR320 [37]	320	350	90	4.8 (tensile) −7 (compressive) 2.1 (shear)		

### 3. Structural Model

The representative structural model is a flat longitudinally framed panel of dimensions 2.4 m × 2.4 m as shown in Figure 4b. A ‘region of interest’ is demarcated in the middle for recording structural response to omit any abnormal stresses developed at boundaries [38].

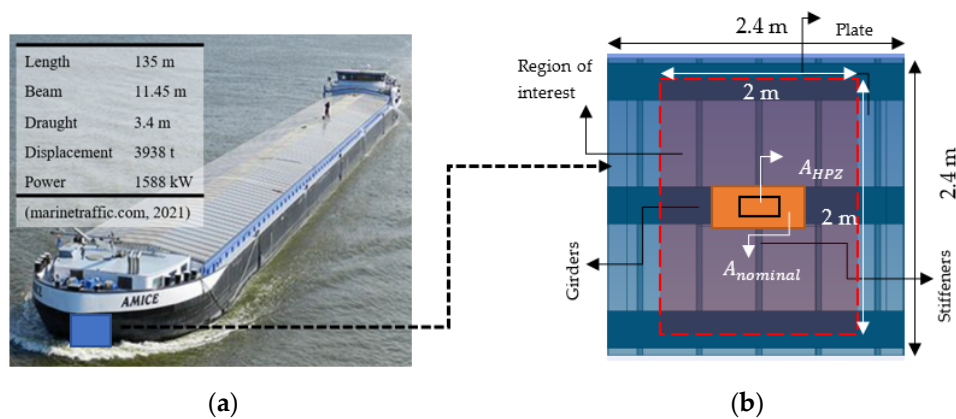


**Figure 4.** A representative inland waterway barge in Lake Mälaren shown in (a) is used as basis to develop a reference hull plate shown in (b).

#### Ice Pressure, Loading Area and Representative Hull Panel

Ice load estimation methods represent the largest source of uncertainty in OTW predictions [29]. We lean towards conservative design and opt for rule-based design. The panel is subjected to quasi-static pressure during the crushing-bending phase in Figure 1a. The magnitude recommended by FSICR [1] is dependent on the vessel displacement ( $\Delta$ ) as seen in Equation (3):

$$p = c_d \cdot c_1 \cdot c_a \cdot P_0 \tag{1}$$

$$c_d = \frac{a \cdot k + b}{1000} \tag{2}$$

$$k = \frac{\sqrt{\Delta \cdot P}}{1000} \tag{3}$$

where,  $P_0$  is the nominal pressure,  $P$  is the engine power and  $c_d, c_l, c_a, a$  and  $b$  are design constants [1].

Since the structural concepts and respective materials in this study vary in density, the target vessel will vary in displacement, leading to different ice pressures. This may create inadequate conditions for comparison. Correspondingly, all vessel variants are taken to have the same displacement assuming that this is managed by adjusting ballast. A barge is ideal in meeting this assumption as its displacement can be varied depending on the volume and density of cargo. Such a barge: M/S Amice is shown in Figure 4a.

Following Equation (1) we calculate the ice-pressure assuming a target ice thickness of 50 cm, corresponding to a 95% operational time window (see Figure 5). This corresponds to a load height of 25 cm and ice-class 1B in FSICR. The predicted nominal ice pressure and high-pressure zone (HPZ) pressure are 1.71 MPa and 3.06 MPa, respectively. This nominal pressure corresponds to IACS [3]’s nominal pressure prediction but the HPZ pressure predicted by FSICR is ~50% higher. Here, we consider the more critical case by FSICR (Table 4).

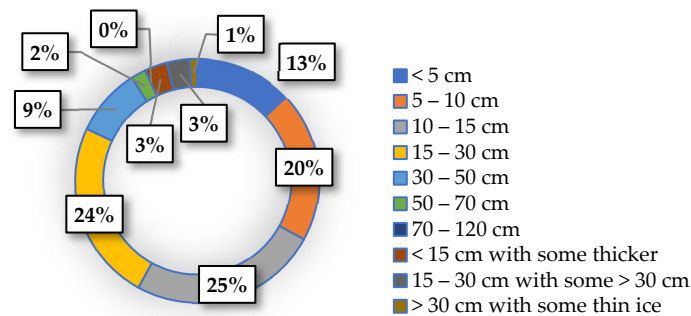


Figure 5. Ice thickness distribution in Lake Mälaren, Sweden between 1983–2017 [39].

Table 4. Pressure due to ice on the hull as calculated by different rules.

Method	Pressure (MPa)	
	Average	Peak
FSICR 1B	1.71	3.06
IACS PC 6	1.71	2.23

The nominal and HPZ pressures are applied in the middle of the panel (Figure 4b), within the ice belt region. A nominal pressure area is defined following IACS [3] rules since it considers simplified plastic response in its formulation, making it more realistic and critical. The HPZ area is sourced from the work performed by Zhang, Cheemakurthy [40] corresponding to loading conditions in Stockholm using a probabilistic approach for a probability of exceedance of 0.01 and number of annual ram events as 1 million. Respective dimensions are shown in Table 5.

Table 5. Dimensions of pressure patches calculated using various approaches.

Method	Pressure Patch	Type
IACS PC 6	0.307 m × 1.02 m	Nominal area
Probabilistic Method	0.096 m <sup>2</sup>	HPZ area

#### 4. Finite Element Model

##### 4.1. Meshing and Elements

ANSYS workbench’s explicit finite element solver is used to simulate the structural response of all candidates. Starting with a coarse mesh, the element size was decreased and refinements were added in critical areas near the load patch until the deformation

converged at  $\sim 1.8$  mm at 1 MPa for a single frame with a T girder corresponding with FE simulation results by Daley and Hermanski [20]. The meshing controls were set to have a minimum elemental quality of 0.25 and the reported aspect ratios were largely under 10 and the Jacobian ratios under 3. The reported stresses were taken as an elemental average over individual bodies to discount for peak stresses arising from inadequate meshing. Stresses at boundaries were not included in the analysis.

For metal grillage, 10-node Tetrahedrons and 20-node Hexahedron solid elements were used (Figure 3a). A lower bound of 2.5 mm was chosen as the mesh element size. The analysis settings were set to describe a linear model with some allowance for non-linear behavior. This was performed from the perspective of improving computational efficiency as we are only interested in the elastic region corresponding to our damage criteria in Section 5. In modeling the sandwich and stiffened sandwich, 4-node linear shell elements were chosen to represent the faces while 8-node solid elements were chosen to represent the core (Figure 3b). The adhesive bonding between the face and core was assumed to be perfect. Considering shell elements are 4-node as compared to solid elements which are 8-node, the savings in computational time are considerable with an accuracy error under 5% [41]. The modeling was performed in ACP in combination with the static structural module in the ANSYS workbench. The analysis settings were set to non-linear. The limiting criteria were set to respective Hashin IRFs outlined in Section 5.

#### 4.2. Boundary Conditions

The boundaries cannot be idealized as fixed or simply supported [42] as one observes displacement normal to the plate and rotations about in-plane axes. However, keeping in line with DNVGL [2]'s recommendations we set  $u_y = u_z = 0$ ;  $r_x = 0$  and  $u_x, r_y$  and  $r_z$  as free. In addition, we apply  $u_x = 0$  to avoid rigid body motion.

#### 4.3. Model Validation

Considering the large number of parametric cases in this study, validating them all with experimental data is practically unfeasible. Instead, we choose to validate the FE model to be as close as possible to experimental data found in the literature.

Daley and Hermanski [20] conducted experiments along with numerical studies to determine the plastic reserve strength of a single frame with a T cross-section girder. Considering only the linear portion of the analysis as a reference, the results from the model in the current study are validated with the numerical and experimental findings [20]. The deflection measured at the frame center presented in Figure 6a is in a qualitatively good agreement when comparing the model in the current study.

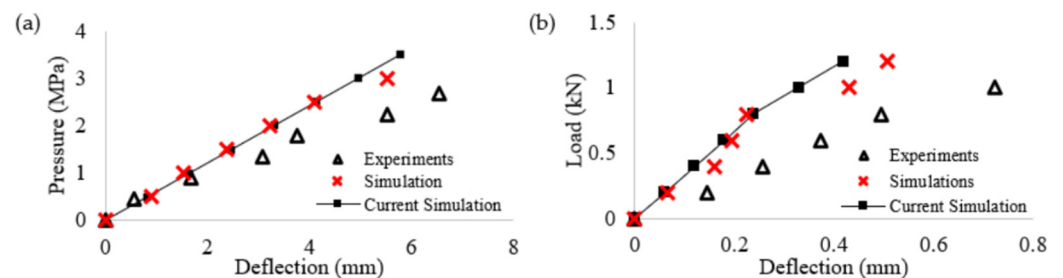


**Figure 6.** Validation of ANSYS model for simulation of quasi-static analysis on (a) metal grillage [20] and (b) sandwich structure [21].

Zhu and Chai [21] conducted experiments to investigate a composite sandwich panel under quasi-static indentation. Considering only the linear portion of the analysis as a reference, the results from the sandwich panel model in the current study are validated with the numerical and experimental results [21] in Figure 6b. The dataset used in our paper includes some uncertainties that account for the differences between experimental and simulation results as mentioned in Zhu and Chai [21].



### 5. Damage Characterization

A summary of criteria for successful candidates is shown in Table 6.

**Table 6.** Criteria for successful candidates. (*b* is taken as the panel span of the region of interest).

Criteria	Limit
Peak stress	<90% of yield stress
Maximum displacement	Metal grillages: $0.01b = 20$ mm [38] Sandwich: $0.02b = 40$ mm [32]
Composite IRFs	0.75–0.95

For quasi-static loading, we may limit damage modes of composites to respective failure criteria defined by Hashin [43] where we compare the stress and strain states of on-axis lamina to its strengths.

#### Hashin Criteria

The Hashin failure criteria [43] are based on physics and describe several failure modes. Tensile fibre failure: ( $\sigma_{11} \geq 1$ )

$$\left(\frac{\sigma_{11}}{X_T}\right)^2 + \frac{\sigma_{12}^2 + \sigma_{13}^2}{S_{12}^2} < 1 \tag{4}$$

Compressive fibre failure: ( $\sigma_{11} < 1$ )

$$\left(\frac{\sigma_{11}}{X_C}\right)^2 < 1 \tag{5}$$

Tensile matrix failure: ( $\sigma_{22} + \sigma_{33} > 0$ ),

$$\frac{\sigma_{22}^2 + \sigma_{33}^2}{Y_T^2} + \frac{\sigma_{23}^2 - \sigma_{22}\sigma_{33}}{S_{23}^2} + \frac{\sigma_{12}^2 + \sigma_{13}^2}{S_{12}^2} < 1 \tag{6}$$

Compressive matrix failure: ( $\sigma_{22} + \sigma_{33} < 0$ )

$$\left[\left(\frac{Y_C}{2S_{23}}\right)^2 - 1\right] \left(\frac{\sigma_{22} + \sigma_{33}}{Y_C}\right) + \frac{(\sigma_{22} + \sigma_{33})^2}{4S_{23}^2} + \frac{\sigma_{23}^2 - \sigma_{22}\sigma_{33}}{S_{23}^2} + \frac{\sigma_{12}^2 + \sigma_{13}^2}{S_{12}^2} < 1 \tag{7}$$

Interlaminar tensile failure: ( $\sigma_{33} > 0$ )

$$\left(\frac{\sigma_{33}}{Z_T}\right)^2 < 1 \tag{8}$$

Interlaminar tensile failure: ( $\sigma_{33} < 0$ )

$$\left(\frac{\sigma_{33}}{Z_C}\right)^2 < 1 \tag{9}$$

For comparing the structural concepts, two new variables *SpW* and *DpW* are introduced to compare the strength and stiffness capacity per mass of the variants. They are adjusted such that only successful candidates have a positive value. For metal grillages, they are expressed as:

$$SpW = \frac{(SSF - 1)}{m} \times 1000 \tag{10}$$

$$DpW = \frac{(DSF - 1)}{m} \times 1000 \tag{11}$$

$$SSF = \frac{90\% \text{ of yield stress}}{\text{maximum observed equivalent stress}} \tag{12}$$

$$DSF = \frac{\Delta_a}{\Delta_r} \tag{13}$$

where,  $SpW$  is the strength per mass rating,  $DpW$  is the stiffness per mass rating,  $SSF$  is the stress safety factor,  $m$  is the geometric mass,  $\Delta_a = 20$  mm, is the allowable deformation and  $\Delta_r$  is the maximum observed deformation.

For sandwich and stiffened sandwich,  $SpW$  is defined as:

$$SpW = \frac{\left(\frac{1}{IRF^2} - 1\right)}{m} \times 1000 \tag{14}$$

where,  $IRF$  is the inverse reserve factor corresponding to  $Z =$  Hashin failure mode and  $m$  is the mass of the structure.  $DpW$  is the same as for metal grillage.

### 6. Results

In this section, we explore three objectives: (a) Identification of lightweight structural concepts for bearing quasi-static ice loads. (b) Identification of sensitive parameters and their interactions for each structural concept. (c) The parametric trends of parameters and interactions.

#### 6.1. Overall Comparison of Structural Concepts

##### 6.1.1. Strength

The SSF comparison of the three structural concepts—metal grillage, sandwich, and stiffened sandwich in Figure 7a with respect to mass shows that the sandwich structure (red dots) is the most weight-efficient option in the safe region. The sandwich panels have the highest strength to mass ratio and are on average ~10 times lighter than metal grillage and 1.5 times lighter than the stiffened sandwich. However, securing this advantage of weight requires the sandwich panel to have impractical large core thicknesses (>240 mm). The thickness limit is established as the web height to the T-stringer scantlings corresponding to FSICR prescribed section modulus for 1B ice class. In the comparison of the three concepts in Figure 7b, the steel grillage (black dots) is the thinnest option followed by the sandwich and stiffened sandwich, within the safe region.

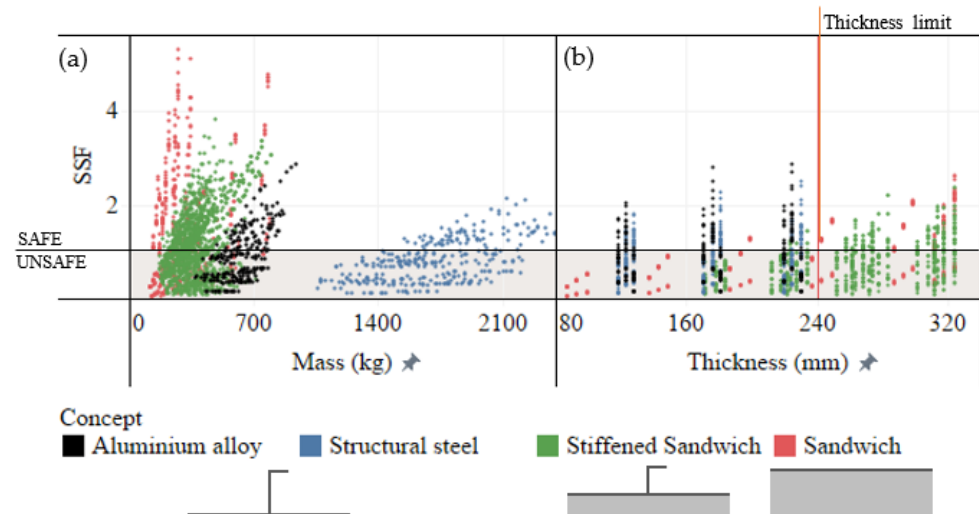
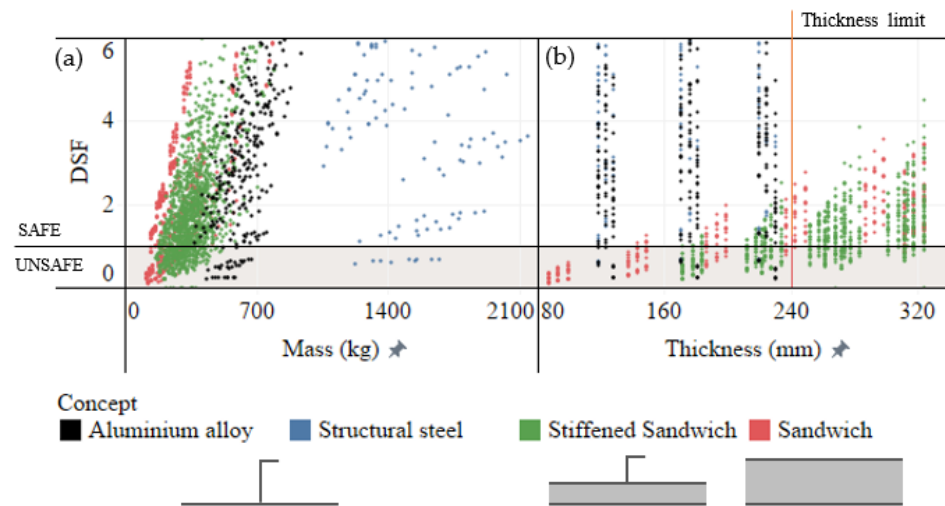


Figure 7. Comparison of stress safety factors with respect to (a) mass and (b) panel thickness for all structural concepts.

### 6.1.2. Stiffness

On comparing DSF in Figure 8a, the sandwich structure (red dots) is the lightest option, followed by the stiffened sandwich and metal grillage. Within the safe region, the steel grillage is ~6 times heavier and a stiffened sandwich is ~1.4 times heavier than a sandwich structure. The sandwich structure has the highest stiffness to mass ratio, followed by the metal grillage and the stiffened sandwich. Under a thickness limit of 240 mm in Figure 8b, the metal grillage is the thinnest option at ~120 mm, followed by the sandwich structure at ~140 mm and stiffened sandwich at ~220 mm.



**Figure 8.** Comparison of deformation safety factors with respect to (a) mass and (b) panel thickness for all structural concepts.

If we compare strength and stiffness with respect to (a) mass and (b) panel thickness < 240 mm, we see that the stiffened sandwich panel offers both (a) low mass and (b) high gross tonnage as shown in Figure 9. This combination makes it appealing as the recommended choice.

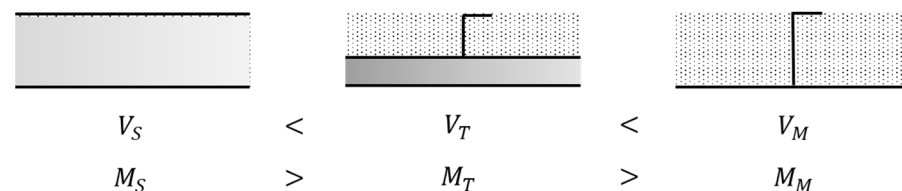


**Figure 9.** Comparison of the three structural concepts shows the order of mass ( $M_x$  and volume occupied ( $V_x$ ) where  $x$  = Sandwich (S), Stiffened sandwich (T) and metal grillage (M).

### 6.1.3. Comparison of Best Variants

In Tables 7 and 8, we compare the parametric combination of best variants along with their masses and  $SpW/DpW$ . Considering strength we observe within metal grillages, the aluminum alloy is ~3 times lighter than steel. For sandwich structures, both C230 and C395 have very similar masses when comparing strengths. Their performance is similar with PVC200 and PET GR200 cores with a slight advantage towards the former core. Considering stiffness, the C395 option is the lightest. The E-glass variant is not a suitable option for sandwich panels. Its mass is larger than the aluminum grillage and it has a core thickness > 450 mm. For stiffened sandwich structure, C395 results in the lightest option in terms of strength. The mass is ~10% larger than its sandwich panel counterpart. The most suitable choice of core material is PET GR200 for both carbon face materials. The E-glass variant shows a viable option within the thickness limit < 240 mm with a PVC60 core and has a mass comparable with the aluminum grillage. In terms of stiffness, all materials enable low mass with C395 being the lightest option.

**Table 7.** Best parametric combinations by material in terms of  $SpW$  and mass.

	Material	Stiffener Spacing (m)	Stringer Spacing (m)	Thickness (m)	Stiffener Z (cm <sup>3</sup> )	Stringer Z (cm <sup>3</sup> )	$SpW$ (MPa/kg)	Eq. Stress (MPa)	Mass (kg)
Metal Grillage	Aluminum	0.25	1	0.015	18	150	0.354	238	495
	Steel	0.25	0.5	0.015	18	150	0.016	211	1738
	Face material	Core material	Ply thickness (mm)	Core thickness (mm)	No. of stiffeners	Stiffener Z (cm <sup>3</sup> )	$SpW$	Hashin IRF	Mass (kg)
Sandwich	C230UD	PVC200/PETGR200	0.4	175	-	-	1.01/0.99	0.79	268
	C395UD	PVC200/PETGR200	0.4	175	-	-	1.08/1.06	0.78/0.77	269
	E-Glass	PVC200	0.4	450	-	-	0.193	0.89	611
Stiffened Sandwich	C230UD	PETGR200	0.3	140	4	18	0.129	0.96	330
	C395UD	PETGR200	0.2	150	3	18	0.35	0.91	295
	E-Glass	PVC60	0.4	150	5	95	0.222	0.89	512

**Table 8.** Best parametric combinations by material in terms of  $DpW$  and mass.

	Material	Stiffener Spacing (m)	Stringer Spacing (m)	Thickness (m)	Stiffener Z (cm <sup>3</sup> )	Stringer Z (cm <sup>3</sup> )	$DpW$ (MPa/kg)	Deformation	Mass (kg)
Metal Grillage	Aluminium	0.67	1	0.01	18	150	0.15	18.9	374
	Steel	0.5	0.67	0.01	18	150	0.09	18	1249
	Face material	Core material	Ply thickness (mm)	Core thickness (mm)	No. of stiffeners	Stiffener Z (cm <sup>3</sup> )	$DpW$	Deformation	Mass (kg)
Sandwich	C230UD	PVC200	0.3	175	-	-	0.968	32.1	253
	C395UD	PVC200	0.4	125	-	-	0.52	36.1	209
	E-Glass	PVC200	0.3	225	-	-	0.34	36	323
Stiffened Sandwich	C230UD	PETGR200	0.2	150	3	18	1.13	30.1	293
	C395UD	PETGR200	0.2	140	3	18	0.53	34.8	283
	E-Glass	PETGR200	0.3	150	3	18	0.191	37.3	379

From the above comparison, we observe that SSF is more critical in comparison with DSF for most parametric variants. This is demonstrated in Tables 7 and 8 where masses of best variants with respect to strength are larger than those with respect to stiffness. Correspondingly we focus on strength as a comparative measure from here on.

### 6.2. Identification of Significant Parameters

To identify significant parameters among those identified in Table 2 we use analysis of variance (ANOVA). The ANOVA model is taken as linear and the condition for rejecting the null hypothesis is a 95% confidence interval or  $p$ -value  $\leq 0.05$  and the  $F > F_{critical}$  in the F distribution table [44].

#### 6.2.1. Metal Grillage

From Table 9, the P-values for plate thickness (M1), material (M2), stiffener Z (M3), stringer Z (M4) and ice stringer (M6) were less than 0.05 and we can conclude that they have a statistically significant influence on the stress safety factor within the selected parametric range. Ice stiffener (M5), stringer spacing (M7) and stiffener spacing (M8) were found as statistically insignificant. M5 denotes there is no significant difference whether the load patch falls on the stiffener or in-between stiffeners. M7 denotes that while an ice stringer is present, the spacing between stringers is not significant in contributing to stress capacity. This implies that most of the strength contribution comes from the ice stringer. M8 denotes that stiffener spacing has a statistically insignificant influence on the stress capacity between 0.25 m and 0.5 m. However, higher stiffener spacings showed statistical significance.

**Table 9.** ANOVA analysis for metal grillage parameters for SSF. Significant parameters are highlighted in bold and underlined. Order of sensitivity is indicated under rank.

Parameter	Symbol	SS	MS	F	$p$ -Value	F Crit	Rank
<b><u>Plate thickness</u></b>	M1	2.97	1.48	5.79	0.003	3.01	3
<b><u>Material</u></b>	M2	2.73	2.73	12.10	0.0005	3.86	1
<b><u>Stiffener Z</u></b>	M3	2.36	2.36	8.44	0.004	3.87	2
<b><u>Stringer Z</u></b>	M4	2.97	1.48	5.79	0.003	3.01	4
Ice Stiffener	M5	0.35	0.35	1.42	0.24	3.9	
<b><u>Ice Stringer</u></b>	M6	1.14	1.14	4.94	0.026	3.87	5
Stringer spacing	M7	0.18	0.18	0.78	0.38	3.9	
Stiffener spacing	M8	1.49	0.74	3.09	0.051	3.11	

#### 6.2.2. Simple Sandwich

From Table 10, parameters ply thickness (S2), core thickness (S3, S4) and face material (S5) have a statistically significant influence on the SSF while factors ply configuration (S1), and core material (S6) are statistically insignificant. Of the three ply-orientations selected, we choose  $[90/0/45/ - 45/45/ - 45/0/90]_s$  for stiffened sandwich as it has the best performance. S6 denotes there is no significant difference between dense core materials for sandwich structures.

**Table 10.** ANOVA analysis for sandwich panel parameters for SSF. Significant parameters are highlighted in bold and underlined. Order of sensitivity is indicated under rank.

Parameter	Symbol	SS	MS	F	$p$ -Value	F Crit	Rank
Ply configuration	S1	0.46	0.23	0.17	0.84	3.02	
<b><u>Ply thickness</u></b>	S2	76.52	38.26	33.38	$2.3 \times 10^{-14}$	3.01	4
<b><u>Light core thickness</u></b>	S3	98.67	49.34	49.08	$4.06 \times 10^{-19}$	3.03	3
<b><u>Dense core thickness</u></b>	S4	22.51	5.63	32.77	$1.98 \times 10^{-21}$	2.41	2
<b><u>Face material</u></b>	S5	22.36	11.18	65.40	$4.66 \times 10^{-23}$	3.04	1
Core material	S6	0.017	0.008	0.03	0.97	3.06	

#### 6.2.3. Stiffened Sandwich

From Table 11, parameters ply thickness (T1), core thickness (T2, T3), face material (T4), core material (T5), stiffener Z (T6) and stiffener spacing (T7) have a statistically significant

influence on the stress safety factor while the presence of a stiffener centered at the pressure patch (T8) is statistically insignificant. Of the statistically significant parameters—in T6, the *p*-value between 18 cm<sup>3</sup> and 57 cm<sup>3</sup> is 0.03 while that between 57 cm<sup>3</sup> and 95 cm<sup>3</sup> is 0.23, indicating that the latter combination is statistically insignificant, and we can opt for the smaller section modulus to save weight. T8 implies the stress capacity on the panel is independent of whether the load acts on or in-between the stiffeners.

**Table 11.** ANOVA analysis for stiffened sandwich parameters for SSF. Significant parameters are highlighted in bold and underlined. Order of sensitivity is indicated under rank.

Parameter	Symbol	SS	MS	F	<i>p</i> -Value	F Crit	Rank
<b><u>Ply thickness</u></b>	T1	47.31	23.66	54.46	$3.02 \times 10^{-71}$	3.002	1
<b><u>Fat core thickness</u></b>	T2	101.31	50.65	175.00	$1.93 \times 10^{-61}$	3.01	2
<b><u>Thin core thickness</u></b>	T3	23.78	11.89	59.09	$8.07 \times 10^{-25}$	3.006	4
<b><u>Face material</u></b>	T4	83.23	41.62	101.26	$4.92 \times 10^{-42}$	3.002	3
<b><u>Core material</u></b>	T5	12.30	6.15	29.80	$3.63 \times 10^{-13}$	3.008	5
<b><u>Stiffener Z</u></b>	T6	71.91	35.95	4.09	0.017	3.002	6
<b><u>Stiffener spacing</u></b>	T7	2.42	1.21	3.19	0.042	3.014	7
Ice stiffener	T8	0.00014	0.00014	0.000824	0.98	3.86	

### 6.3. Influence of Parametric Interactions

The statistical significance of the interactions between significant parameters on the stress-bearing capacity are investigated using a 2<sup>n</sup> factorial design of experiment (DOE). The study of interactions is a necessary step in parametric explorations [45]. Interactions between three or more parameters are not included here.

For metal grillages, we omit the interaction with the ice stringer (M6) because from Figure 10 it is evident that in the absence of an ice stringer, the structure fails in most cases. Considering only those cases with an ice stringer, the number of statistically significant interacting parameters get reduced to M1, M2, M3 and M4. The resulting DOE table showed that there are no significant interactions. Similarly for the sandwich structure, if we consider only high-density cores, our significant parameters get limited to S2, S4 and S5 for which we find no significant interactions.

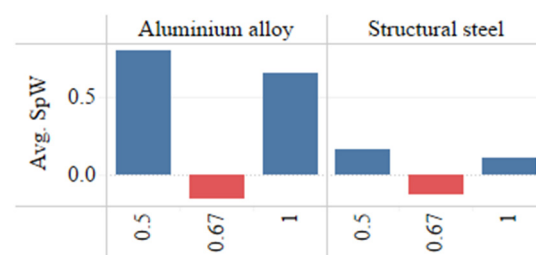


**Figure 10.** Effect of having an ice stringer vs. no ice stringer on the SSF of a metal grillage.

For the stiffened sandwich, if we only consider high-density cores, significant parameters get reduced to ply thickness (T1), thin core thickness (T3), face material (T4), core material (T5), stiffener section modulus (T6) and number of stiffeners (T7). From Table 12, we find several significant interactions (indicated in red). Of these interactions, three of them consist of ‘core material’. We simplify by assuming a fixed core of PET GR200 considering it was the best performer in Table 7 and can hereby omit T3T5, T5T6 and T5T7. The resulting interactions are shown in Table 12.

**Table 12.** Statistical significance of interaction between sandwich panel parameters. Statistically significant interactions are highlighted in bold and underlined. The omitted interactions are marked with a strikethrough.

Interaction	SS	MS	F	p-Value	Interaction	SS	MS	F	p-Value
T1T3	0.035	0.035	1.671	0.203	T3T6	0.009	0.009	0.406	0.528
T1T4	0.052	0.052	2.497	0.122	<b><u>T3T7</u></b>	0.563	0.563	26.810	0.000
T1T5	0.050	0.050	2.386	0.130	<b><u>T4T5</u></b>	0.306	0.306	14.579	0.000
<b><u>T1T6</u></b>	0.124	0.124	5.922	0.019	T4T6	0.044	0.044	2.085	0.156
T1T7	0.007	0.007	0.324	0.572	T4T7	0.042	0.042	1.980	0.167
T3T4	0.047	0.047	2.218	0.144	<b><u>T5T6</u></b>	0.239	0.239	11.389	0.002
<b><u>T3T5</u></b>	0.134	0.134	6.377	0.015	<b><u>T5T7</u></b>	1.038	1.038	49.404	0.000
<b><u>T6T7</u></b>	0.139	0.139	6.617	0.014					

6.4. Parametric Trends of Significant Parameters and Interactions

6.4.1. Parametric Trends

For metal grillages, we observe the influence of significant parameters on the SSF in Figure 11. Plate thickness [M1], stiffener spacing [M8], and material [M2] have the largest sensitivity. The circles in red indicated for stringer [M4] and stiffener section modulus [M3] are parametric values at which there is no significant gain in SSF and represent a potential area for weight savings. This implies one can opt for a stringer and stiffener section modulus of 303 cm<sup>3</sup> and 57 cm<sup>3</sup>. Since we observed no statistical significance between loads acting on or in between stiffeners, one can opt for a stiffener spacing of 0.67 to have maximum weight savings.

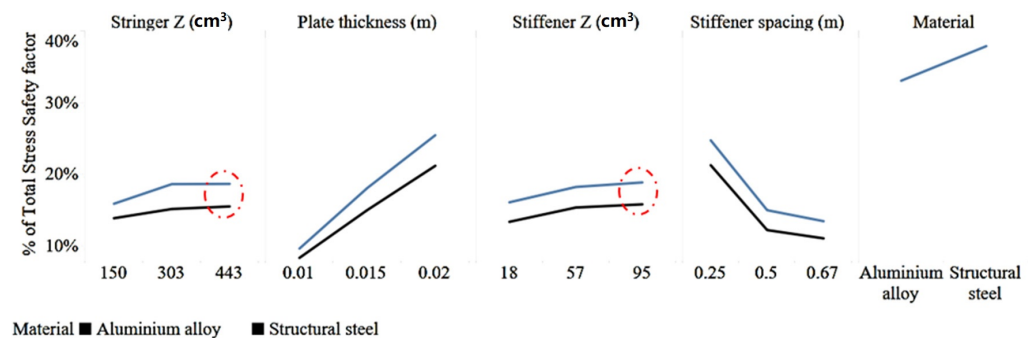


**Figure 11.** Parametric trend of significant parameters for metal grillage.

For sandwich structures, the parametric variation of significant parameters is shown in Figure 12. Both high-density [S4] and low-density cores [S3] have large statistical significance at a low thickness range. For face materials [S5], there is statistical insignificance between C230UD and C395UD variants. From an economical perspective, C230UD is favorable.

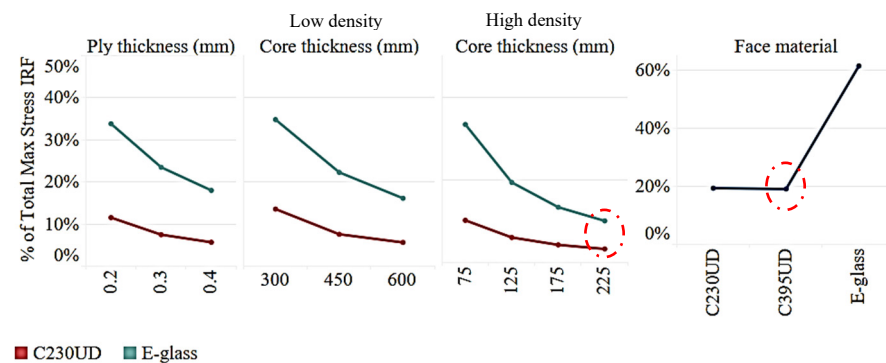


**Figure 12.** Sensitivity Analysis of parameters for sandwich panel stress safety factor.

For stiffened sandwich structures, the parametric influence of significant parameters is shown in Figure 13. For low-density core materials [T4] and stiffener spacing of 0.5 m–0.67 m for C230UD face sheet [T7], we observe no statistical significance. All other parameters are statistically significant with ply [T1] and core thickness [T2, T3] and face material [T4] being the most sensitive.

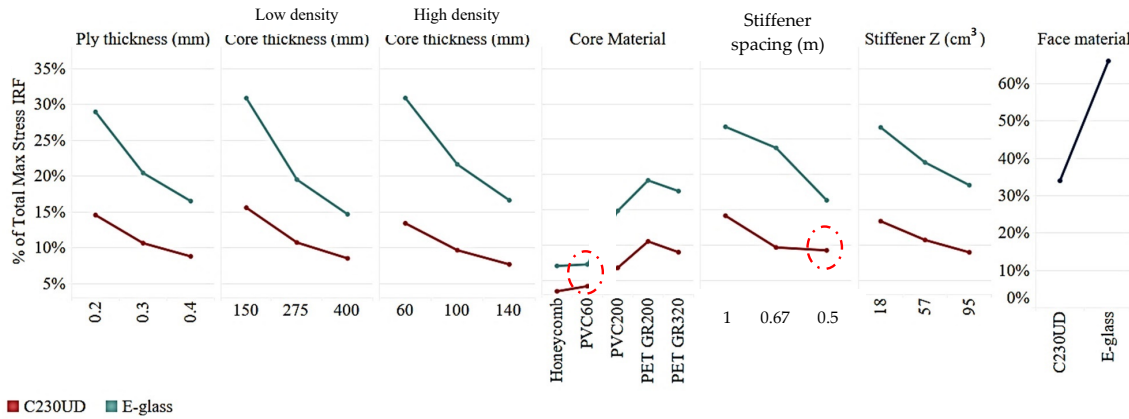


Figure 13. Sensitivity analysis of parameters for stiffened sandwich panel stress safety factor.

#### 6.4.2. Interactions

We observed interactions only for the stiffened sandwich structure. Figure 14 compares the influence of face and core material on Hashin strength criteria, representing the interaction–T4T5. The interaction signifies there is a difference in performance for different combinations of face and core materials. PVC 200 is found to be the most suitable core material offering the lowest weight while having core thickness < 240 mm. The viable pool of E-glass variants denoted by a dotted boundary is ~2 times heavier than the carbon fibre counterpart.

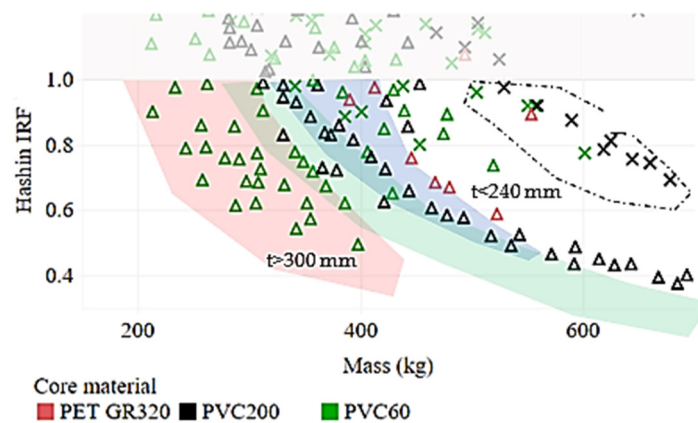
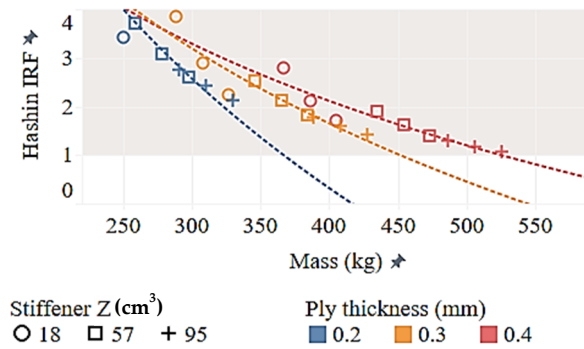


Figure 14. Interaction T4T5–Influence of face and core materials on Hashin failure criteria. The orange patch denotes low-density core while blue patches denote high-density cores. The triangles represent carbon fiber face sheets while crosses represent E-glass face sheets.

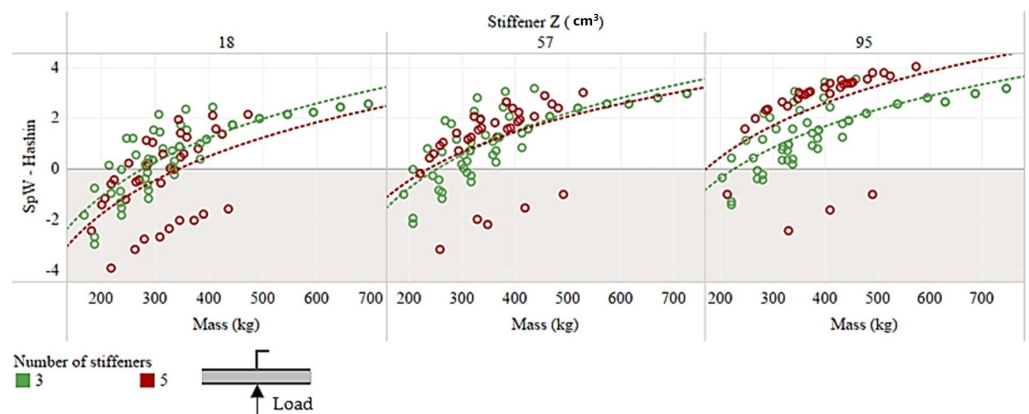
Figure 15 shows the influence of face thickness with respect to stiffener section modulus representing the interaction T1T6 for E-glass having a PET GR200 core. The interaction implies that the strength gain due to larger stiffeners is more effective at a higher ply thickness. The general trend for different ply thicknesses shows a shift towards the right with an increase in the stress capacity. Through regression, we can identify the ply thickness for a viable E-glass variant.





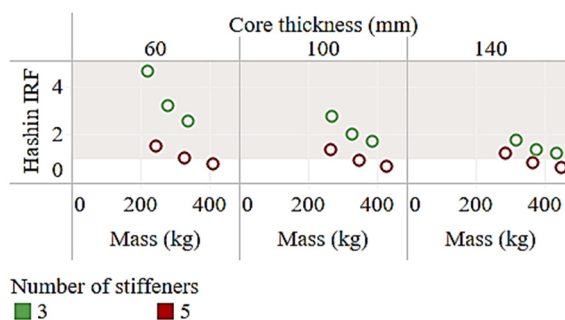
**Figure 15.** Influence of face ply thickness and stiffener section modulus. The stiffener section modulus are denoted by symbols while ply thickness values are denoted by colors.

Figure 16 shows the influence of the number of stiffeners and stiffener section modulus' (interaction T6T7) on Hashin failure criteria. In general, we observe that *SpW* increases with stiffener section modulus. However, as the stiffener section modulus increases, the 3-stiffener arrangement loses its low weight advantage in favor of the strength gain offered by the 5-stiffener arrangement. The difference between a 3 and 5-stiffener arrangement is minimal at the mean parametric range of section modulus.



**Figure 16.** The influence of number of stiffeners on the stiffener section modulus against Hashin criteria. Red represents a 3 stiffener configuration and green represents a 5 stiffener configuration.

Figure 17 shows the interaction between core thickness and number of stiffeners representing T3T7. We note a decrease in the advantage gained by having more stiffeners as the core thickness increases. Essentially, the design is converging towards a sandwich panel. Hereby, to save mass, it is of advantage to opt for a lower number of stiffeners with higher section modulus.



**Figure 17.** Influence of core thickness on the no. of stiffeners in the assessment of Hashin criteria. Red represents a 3 stiffener configuration and green represents a 5 stiffener configuration.

### 7. Discussion

In this study, we parametrically analyzed metal grillages, sandwich panels and stiffened sandwich panels using a commercial finite element software for rule-based strength and stiffness compliance representative of operations in thin first-year ice. Some points of discussion are presented here.

In metal grillages, the central girder and plate thickness carry most of the stresses. However, as the plate thickness increases, contribution from the plate and central girder is comparable to contribution from stiffeners. The side girders contribute very little to the overall strength. This motivates one to have side girders with large girder spacing or low section modulus as a means to reduce weight. Figure 18 shows this behavior for steel and aluminum where we see stresses at different grillage components. Aluminum has a higher strength/mass ratio, making it more practical to strengthen the vessel.

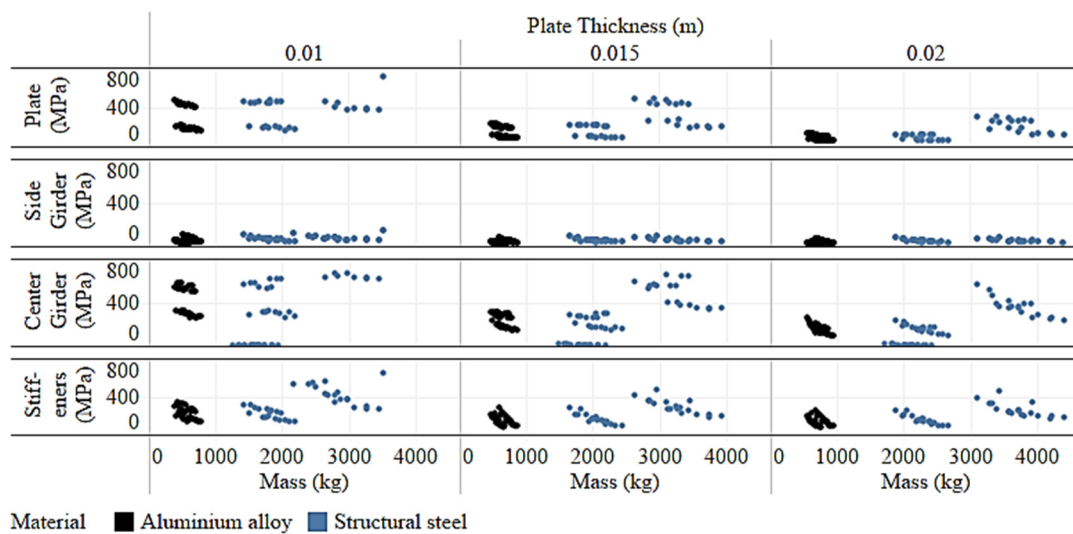


Figure 18. Contribution from different structural elements of a metal grillage towards strength.

If we look at the distribution of variants with respect to mass for sandwich panels, then we find for a given ply thickness, the variants follow a logarithmic distribution as seen by the dotted red line in Figure 19. This information can be used to estimate  $SpW$  at higher scantlings. The higher strength/mass ratio of carbon fibre (red dashed line) is indicated by a steeper curve in comparison with E-glass (blue dashed line).

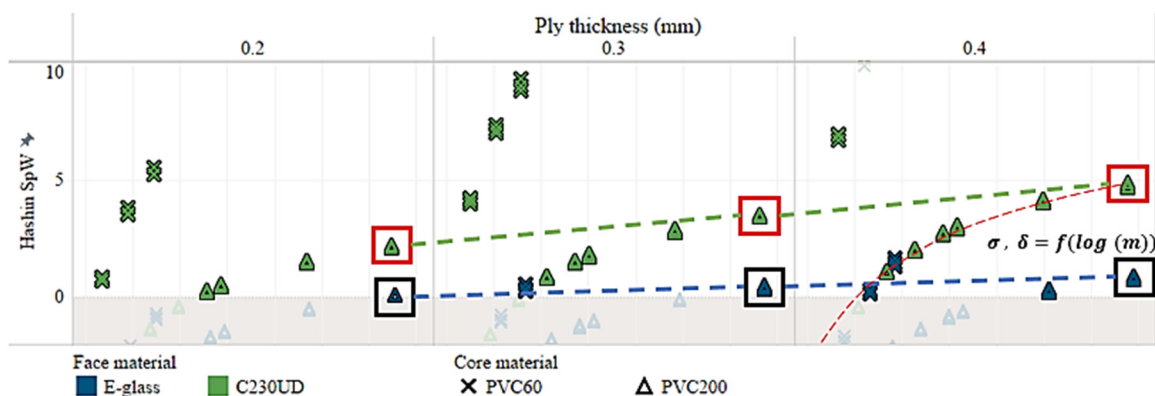


Figure 19. The influence of ply thickness on the Hashin failure criteria. The red square boxes indicate carbon fibre face sheet while the black square boxes indicate E-glass. Face material are denoted by colour while core materials are denoted by symbols.

It is of interest to compare closed foam cell core materials–PVC and PET. A comparison of core shear failure for sandwich structures shown in Figure 20, places PVC200 as the

better performer due to its comparatively higher shear strength than PET. However, the face sheet IRFs were similar with both cores.

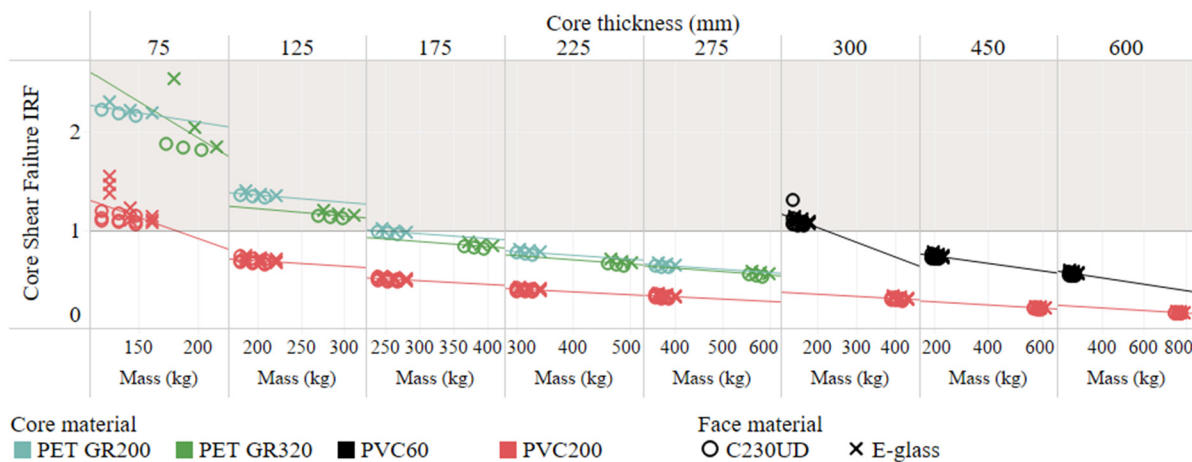


Figure 20. Comparison of core materials on the core shear failure for a sandwich panel.

For sandwich structures, we compare the performance of woven and UD carbon fibre face sheets. From Figure 21a, the woven fibre performs better than UD fibre at low masses but as the mass increases, the difference is negligible. The performance of the UD fibres is sensitive to fibre direction as seen in Figure 21b which may be optimized depending on the applied load. Since ice loads are stochastic in nature, it was observed that woven faces sheets performed better in general.

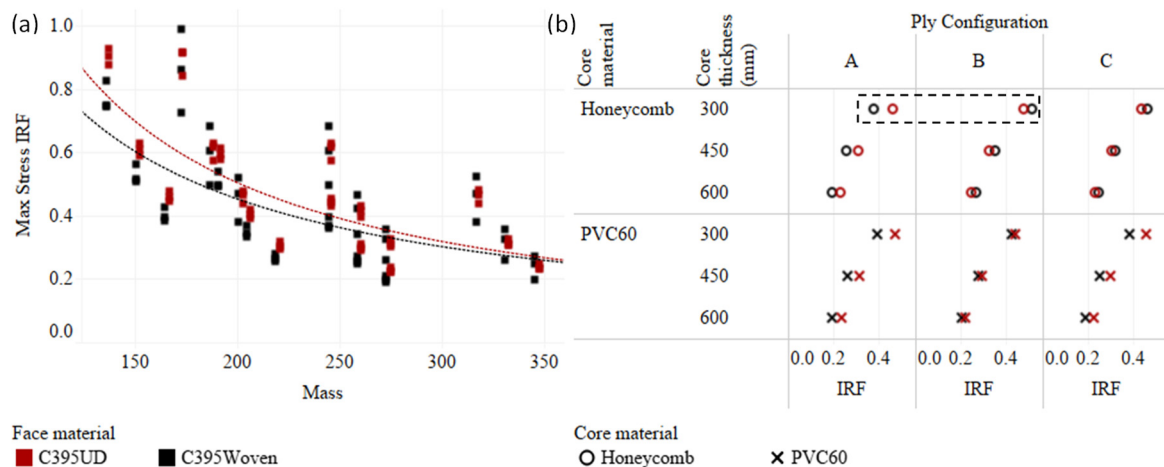
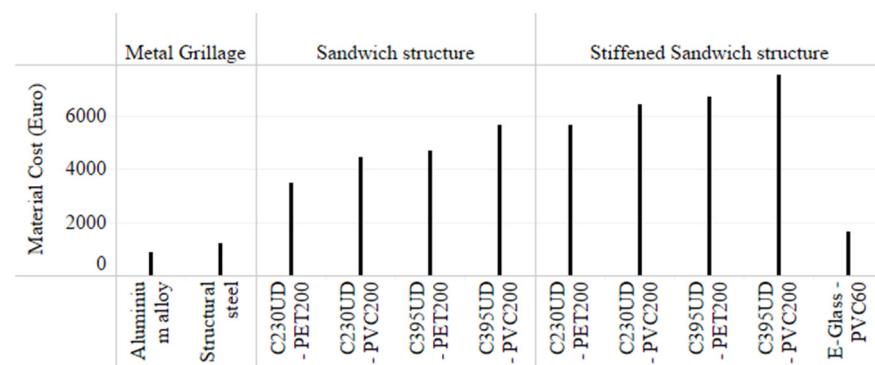


Figure 21. (a) Comparison of strength performance between UD and woven fibres. (b) The black box shows the preference for UD or woven is dependent on the ply configuration.

Out of practical interest, the material costs of the three concepts are compared in Figure 22 for the best variants identified in Table 7. Manufacturing process costs are not included in the comparison. We see that metal grillages are the most economical. Among them, the lightweight aluminum grillage costs are lower despite a ~2.5 times higher material cost. Among composites, the stiffened sandwich is more expensive in general considering a larger use of face material. The combination with PVC200 is the most economical. We also notice a significant difference in costs between C230UD and C395UD while the difference in their performance is minimal. This might motivate manufacturers to opt for C230 instead.



**Figure 22.** Cost comparison of structural concepts. (The material cost data is sourced from Ansys Granta [32]).

Some limitations with respect to the study are:

- The pressure patch in this case is idealized as a rectangle with dimensions chosen as per rules and there can be differences due to this [46].
- The division of the ice–hull interaction into three independent processes is an idealization. In real life, the phases may overlap resulting in the non-realization of the quasi-static assumption.
- The geometry of the stiffeners on the stiffened sandwich structure is chosen to mimic the metal grillage stiffeners. The concept is based on theoretical investigations by Goel, Matsagar [18]. However, such a geometric arrangement’s practical implementation needs to be investigated as such stiffeners are not usually found in practice in marine vessels. Recent advances in additive manufacturing for composites could be the way [47].

The study resulted in a pool of parametric variants that fulfil the quasi-static loading representative of the bending phase of ice-hull interaction. The viable set of variants will serve as a starting pool towards the investigation of impact loading as part of ice-hull interaction. Together they will contribute towards the development of a lightweight ice-going hull for operations in inland waterways.

The objective of a lightweight ice-going hull is particularly valuable within the context of waterborne public transportation of commuters and in transporting cargo on barges in ice-prone regions like Sweden. By ensuring a lightweight hull, operations can carry on all year-round without the penalty of additional fuel consumption during ice-free months. This will improve passenger perception by boosting reliability [48,49] and improve environmental friendliness and operational costs [50] for operators of ferry services. This may lead to a potential change in perception towards waterborne public transportation held by the public transport providers [51].

## 8. Conclusions

In this study, light-weight structural concepts in addition to classification society prescribed steel metal grillage are studied under quasi-static pressure loading representing thin first-year level ice. The investigated lightweight concepts include aluminum metal grillage, glass and carbon fibre sandwich structures and stiffened sandwich structures with PET and PVC cores. The concepts are investigated parametrically for rule-based strength and stiffness compliance using the finite element method. Significant parameters and their trends and interactions were identified. Good agreement was obtained between the numerical predictions and experimental results on comparing the model accuracy. From the cases studied, the following conclusions can be drawn:

- The stiffened sandwich was identified as the most suitable concept because it offers a combination of high gross tonnage and a light weight. Considering only weight as a metric, sandwich structures were the lightest alternative within thickness limits.

- For the metal grillage, plate thickness, material, stiffener and stringer section modulus and location of stringer are identified as statistically significant parameters. For the sandwich structure, significant parameters are face thickness, core thickness and face material. For the stiffened sandwich, face thickness, core thickness, face and core materials, stiffener section modulus and stiffener spacing are significant.
- For the metal grillage, a stringer's presence in the ice belt region was identified as a critical factor.
- We observe no statistical significance in stiffeners' location with respect to the pressure patch.
- Both carbon fibre and E-glass exhibited viable alternatives for the stiffened sandwich whereas only carbon fibre alternatives were suitable for sandwich structures within the thickness limits.

The broad aim of the study is to lead towards the development of a lightweight hull suitable for vessels operating both in ice and open water. The work performed here helped in creating a pool of viable structural combinations for the quasi-static loading phase. A similar assessment, when performed considering the impact-crushing phase of ice–hull interaction will lead to another pool of viable structural combinations. Together they can lead to the development of a lightweight composite hull that is strong enough to withstand ice operations while being lightweight. This will make it competitive during ice-free periods with non-ice vessels and alternative modes, leading to more efficient mobility with year-round operability that is environmentally sustainable.

**Author Contributions:** Conceptualization, H.C., K.G. and M.B.; methodology, H.C. and Z.B.; software, H.C.; validation, H.C. and Z.B.; formal analysis, H.C.; investigation, H.C.; resources, M.B. and K.G.; data curation, H.C. and Z.B.; writing—original draft preparation, H.C.; writing—review and editing, H.C., Z.B. and K.G.; visualization, H.C. and Z.B.; supervision, Z.B., M.B. and K.G.; project administration, K.G.; funding acquisition, K.G. All authors have read and agreed to the published version of the manuscript.

**Funding:** The Swedish Transport Administration is acknowledged for financially supporting the research program Waterborne Urban Mobility TRV 2018/6471.

**Institutional Review Board Statement:** Not applicable.

**Informed Consent Statement:** Not applicable.

**Data Availability Statement:** The data presented in this study are available on request from the corresponding author.

**Conflicts of Interest:** The authors declare no conflict of interest.

## References

1. *Finnish Swedish Ice Class Rules (FSICR)*; Contract No.: TRAFI/708629/03.04.01.01/2018; Finnish Transport and Communication Agency (Traficom): Helsinki, Finland, 2017.
2. DNV GL. *Rules for Classification—Ships*; Part 6 Additional Class Notations; Chapter 6 Cold Climate; DNV GL: Bærum, Norway, 2015.
3. IACS. *UR I2 Structural Requirements for Polar Class Ships 2019*; Contract No.: UR I2 Rev4 CLN; IACS: Hamburg, Germany, 2019.
4. Pavic, M.; Daley, C.; Hussein, A.; Hermanski, G. *Ship Frame Research Program—A Numerical Study of the Capacity of Single Frames Subject to Ice Load*; OERC Report; Institute for Ocean Technology NRC: St. John's, NL, Canada, 2004; Volume 2.
5. Daley, C.; Hermanski, G. *Ship Frame Research Program—An Experimental Study of Ship Frames and Grillages Subjected to Patch Loads, Volume 1—Data Report*; SSC Project SR. 2008:2008-001; Ship Structure Committee: Washington, DC, USA, 2008.
6. Cheemakurthy, H.; Zhang, M.; Garne, K.; Barsoum, Z. (Eds.) Nonlinear Finite Element Analysis of Inland-Waterway Barge in Fresh Water Ice Conditions. In *Proceedings of the 29th International Ocean and Polar Engineering Conference, Honolulu, HI, USA, 16–21 June 2019*; OnePetro: Richardson, TX, USA, 2019.
7. Abraham, J. Plastic Response of Ship Structure Subject to Ice Loading. Master's Thesis, Memorial University of Newfoundland, St. John's, NL, Canada, 2008.
8. Avellan, T. Weight Estimation of Ice Strengthened Hull Structures. Master's Thesis, Aalto University, Espoo, Finland, 2020.
9. Kujala, P.; Goerlandt, F.; Way, B.; Smith, D.; Yang, M.; Khan, F.; Veitch, B. Review of risk-based design for ice-class ships. *Mar. Struct.* **2019**, *63*, 181–195. [[CrossRef](#)]
10. Crum, K.A.; McMichael, J.; Novak, M. (Eds.) Advances in Aluminum Relative to Ship Survivability. In *Proceedings of the American Society of Naval Engineers Day 2012 Conference, Arlington, VA, USA, 9–10 February 2012*; Citeseer: Princeton, NJ, USA, 2012.

11. Herrnring, H.; Kubiczek, J.M.; Ehlers, S.; Niclasen, N.O.; Burmann, M. Experimental investigation of an accidental ice impact on an aluminium high speed craft. In *Progress in the Analysis and Design of Marine Structures*; CRC Press: Boca Raton, FL, USA, 2017; pp. 697–704.
12. Kujala, P.; Klanac, A. Steel sandwich panels in marine applications. *Brodogr. Teor. Praksa Brodogr. Pomor. Teh.* **2005**, *56*, 305–314.
13. Mouritz, A.P.; Gellert, E.; Burchill, P.; Challis, K. Review of advanced composite structures for naval ships and submarines. *Compos. Struct.* **2001**, *53*, 21–42. [[CrossRef](#)]
14. Lin, C.-C.; Lin, C.-M.; Huang, C.-C.; Lou, C.-W.; Meng, H.-H.; Hsu, C.-H.; Lin, J.H. Elucidating the design and impact properties of composite nonwoven fabrics with various filaments in bulletproof vest cushion layer. *Text. Res. J.* **2009**, *79*, 268–274. [[CrossRef](#)]
15. Zenkert, D.; Shipsha, A.; Persson, K. Static indentation and unloading response of sandwich beams. *Compos. Part B* **2004**, *35*, 511–522. [[CrossRef](#)]
16. Kortenoeven, J.; Boon, B.; de Bruijn, A. Application of sandwich panels in design and building of dredging ships. *J. Ship. Prod. Des.* **2008**, *24*, 125–134. [[CrossRef](#)]
17. Sujiatanti, S.; Zubaydi, A.; Budipriyanto, A. (Eds.) Finite element analysis of ship deck sandwich panel. In *Applied Mechanics and Materials*; Trans Tech Publications Ltd.: Bäch, Switzerland, 2018; Volume 874, pp. 134–139. [[CrossRef](#)]
18. Goel, M.D.; Matsagar, V.A.; Marburg, S.; Gupta, A.K. Comparative performance of stiffened sandwich foam panels under impulsive loading. *J. Perform. Constr. Facil.* **2013**, *27*, 540–549. [[CrossRef](#)]
19. Riska, K.; Bridges, R. Limit state design and methodologies in ice class rules for ships and standards for Arctic offshore structures. *Mar. Struct.* **2019**, *63*, 462–479. [[CrossRef](#)]
20. Daley, C.; Hermanski, G. *Ship Frame/Grillage Research Program—Investigation of Finite Element Analysis Boundary Conditions*; Memorial University OERC Report; National Research Council: Ottawa, ON, Canada, 2005; Volume 2.
21. Zhu, S.; Chai, G.B. Damage and failure mode maps of composite sandwich panel subjected to quasi-static indentation and low velocity impact. *Compos. Struct.* **2013**, *101*, 204–214. [[CrossRef](#)]
22. Daley, C.; Riska, K. *Review of Ship-Ice Interaction Mechanics*; Report from Finnish-Canadian Joint Research Project no. 5, 'Ship Interaction with Actual Ice Conditions'; Interim Report on Task 1a; Helsinki University of Technology: Helsinki, Finland, 1990.
23. Trends in the Ice Physical Properties in Lake Mälaren, Sweden. 2018. Available online: <https://www.smhi.se/en/services/professional-services/scandinavian-waters/swedish-ice-service-1.8715> (accessed on 10 January 2018).
24. Valanto, P. The resistance of ships in level ice. *SNAME Trans.* **2001**, *109*, 53–83.
25. Enkvist, E.; Varsta, P.; Riska, K. (Eds.) The ship-ice interaction. In *Proceedings of the POAC 79, 5th International Conference on Port and Ocean Engineering under Arctic Conditions*, Trondheim, Norway, 13–18 August 1979.
26. Jordaan, I.J. Mechanics of ice–structure interaction. *Eng. Fract. Mech.* **2001**, *68*, 1923–1960. [[CrossRef](#)]
27. Rinsberg, J.W.; Andrić, J.; Heggelund, S.E.; Homma, N.; Huang, Y.T.; Jang, B.S.; Jelovica, J.; Kawamura, Y.; Lara, P.; Sidari, M. (Eds.) Quasi-static response. In *Proceedings of the 20th International Ship and Offshore Structures Congress (ISSC 2018) Volume 3: Discussions*; IOS Press: Amsterdam, The Netherlands, 2020.
28. Wang, B.; Yu, H.-C.; Basu, R. (Eds.) Ship and ice collision modeling and strength evaluation of LNG ship structure. In *Proceedings of the International Conference on Offshore Mechanics and Arctic Engineering, Estoril, Portugal, 15–20 June 2008*; American Society of Mechanical Engineers (ASME): New York, NY, USA, 2008. [[CrossRef](#)]
29. Cheemakurthy, H.; Zhang, M.; Garne, K.; Burman, M.; Ehlers, S.; von Bock und Polach, R.U. Statistical estimation of uncertainties associated with ship operations in fresh water ice. In *Proceedings of the 28th International Ocean and Polar Engineering Conference, Sapporo, Japan, 10–15 June 2018*; OnePetro: Richardson, TX, USA, 2018.
30. DNV GL. *Rules for Classification: Inland Navigation Vessels (RU-INV)*; DNV GL: Bærum, Norway, 2017.
31. Ghiasi, H.; Pasini, D.; Lessard, L. Optimum stacking sequence design of composite materials Part I: Constant stiffness design. *Compos. Struct.* **2009**, *90*, 1–11. [[CrossRef](#)]
32. DNV GL. *Rules for Classification of High Speed, Light Craft and Naval Surface Craft*; Det Norske Veritas: Bærum, Norway, 2015.
33. Ansys. *Material Database: Ansys Granta EduPack Software*; ANSYS, Inc.: Cambridge, UK, 2021.
34. ASME. *ASME BPV Code, Section 8, Div 2, Table 5-110.1*; American Society of Mechanical Engineers (ASME): New York, NY, USA, 1998.
35. Amancio-Filho, S.T.; Camillo, A.P.; Bergmann, L.; Dos Santos, J.F.; Kury, S.E.; Machado, N.G. MIL Military Handbook: MIL-HDBK-5H-Metallic Materials and Elements for Aerospace Vehicle Structures MIL Military Handbook: MIL-HDBK-5H-Metallic Materials and Elements for Aerospace Vehicle Structures, 8-11, 1998. *Mater. Trans.* **2011**, *52*, 985–991. [[CrossRef](#)]
36. Topolo. Parameters of T-C Series Thermo Panel PVC Foam Core. Available online: <http://www.topolocfrt.com/thermo-panel-pvc-foam-core/> (accessed on 19 February 2022).
37. Armacell. *Technical Data: ArmaPET Struct GR. 2021*; Report No.: 00481 | Arma PET Struct I ArmaPET I C\_TDS I 082021 I Global I EN Master; Armacell: Luxembourg, 2021.
38. DNV GL. *Rules for Classification—Ships. Part 3 Hull. Chapter 4 Loads*; DNV GL: Bærum, Norway, 2017.
39. SMHI. *Statistics on Freshwater Ice in Sweden*; Swedish Meteorological and Hydrological Institute: Norrköping, Sweden, 2021.
40. Zhang, M.; Cheemakurthy, H.; Ehlers, S.; Franz von Bock und Polach, R.U.; Garne, K.; Burman, M. Ice pressure prediction based on the probabilistic method for ice-going vessels in inland waterways. *J. Offshore Mech. Arct. Eng.* **2019**, *141*, 021501. [[CrossRef](#)]
41. Feng, G.-Q.; Li, G.; Liu, Z.-H.; Niu, H.-L.; Li, C.-F. Numerically simulating the sandwich plate system structures. *J. Mar. Sci. Appl.* **2010**, *9*, 286–291. [[CrossRef](#)]

42. Yang, B.; Wang, D. Buckling strength of rectangular plates with elastically restrained edges subjected to in-plane impact loading. *Proc. Inst. Mech. Eng. Part C: J. Mech. Eng. Sci.* **2017**, *231*, 3743–3752. [[CrossRef](#)]
43. Hashin, Z. Failure criteria for unidirectional fibre composites. *J. Appl. Mech.* **1980**, *47*, 329–334. [[CrossRef](#)]
44. Taguchi, G.; Elsayed, E.A.; Hsiang, T.C. *Quality Engineering in Production Systems*; McGraw-Hill College: New York, NY, USA, 1989.
45. Bergman, B. *Industriell Försöksplanering Och Robust Konstruktion*; Studentlitteratur: Lund, Sweden, 1992.
46. Kubiczek, J.M.; Andresen-Paulsen, G.; Herrnring, H.; von Bock Und Polach, F.; Ehlers, S. Development of a design load patch for the consideration of ice loads. *Ships Offshore Struct.* **2020**, *15*, S20–S28. [[CrossRef](#)]
47. Parandoush, P.; Lin, D. A review on additive manufacturing of polymer-fibre composites. *Compos. Struct.* **2017**, *182*, 36–53. [[CrossRef](#)]
48. Cheemakurthy, H.; Tanko, M.; Garme, K. *Urban Waterborne Public Transport Systems: An Overview of Existing Operations in World Cities*; Contract No.: 1651-7660; TRITA-AVE 2017:92.; KTH Royal Institute of Technology: Stockholm, Sweden, 2018; ISBN 978-91-7729-648-5.
49. Tanko, M.; Cheemakurthy, H.; Kihl, S.H.; Garme, K. Water transit passenger perceptions and planning factors: A Swedish perspective. *Travel Behav. Soc.* **2019**, *16*, 23–30. [[CrossRef](#)]
50. Cheemakurthy, H.; Garme, K. Fuzzy AHP based design performance index for evaluation of ferries. *Sustainability* **2022**, *14*, 3680. [[CrossRef](#)]
51. Cheemakurthy, H.; Garme, K. A modularly tailored commuter ferry platform. *Int. Shipbuild. Prog.* **2022**, *accepted for publication*.